Modeling Turbidity in a Water Supply Reservoir: Advancements and Issues

Rakesh K. Gelda[1] and Steven W. Effler[2]

Abstract: The development and testing of a "turbidity" model is documented for a water supply reservoir, Schoharie Reservoir, NY, where inorganic terrigenous particles received during runoff events in turbid density currents from the primary tributary cause distinct periodic degradation. The model state variables are fractions (two or three) of the beam attenuation coefficient at 660 nm ($\mathbf{c}_{660}$), a surrogate optical metric of turbidity. The fractions of $\mathbf{c}_{660}$ correspond to slow and rapidly settling components; the latter implicitly accommodates particle aggregation. The transport framework is a two-dimensional (laterally averaged), independently tested, hydrodynamic model. Model testing is supported by detailed measurements of the dynamics of tributary and meteorological drivers and $\mathbf{c}_{660}$ within the reservoir, during and following twelve runoff events. The model is demonstrated to meet the demanding temporal and spatial predictive needs of water supply lakes and reservoirs, by performing well in simulating the timing and magnitude of $\mathbf{c}_{660}$ peaks, the vertical and longitudinal patterns of $\mathbf{c}_{660}$, diminishment following runoff events, and the dependence of impact on magnitude of a runoff event. Further advancements in turbidity modeling, including multiple particle size classes as state variables and explicit representation of particle aggregation and resuspension inputs, are considered.

DOI: 10.1061/(ASCE)0733-9372(2007)133:2(139)

CE Database subject headings: Water supply; Reservoirs; New York; Runoff.

Introduction

Suspended inorganic particles, a component of tripton (inanimate particles; Wetzel 2001), play important roles in a number of processes in aquatic ecosystems by presenting reactive surfaces (James et al. 1997), influencing metabolic activity (Phlips et al. 1995), contributing to net sedimentation (Effler and Matthews 2004), and attenuating light (Kirk 1994; Effler et al. 2002). High concentrations of these inorganic particles in the water columns of water supply lakes and reservoirs are of particular concern because of, for example, esthetic impairments manifested as high "turbidity" levels. This turbidity is attributable to the light attenuating process of scattering; the intensity of this process is quantified by the magnitude of the scattering coefficient (**b**, m^{-1}; Kirk 1994). Features of the particle population that determine **b** include the concentration of particles, their composition, size distribution and shape (Davies-Colley et al. 1993; Kirk 1994). Direct measurements of **b** are rarely available (Davies-Colley and Smith 2001); most of these have been reported for marine systems (e.g., Babin et al. 2003). However, multiple surrogate metrics of **b** exist (Kirk 1994). The measure of choice for the regulatory community in the United States is turbidity [T_n, nephelometric turbidity unit (NTU)] as measured by a turbidimeter (Letterman et al. 2004). These instruments measure light scattered by particles from a beam collected within a rather wide angle centered on 90° (Kirk 1994; Davies-Colley and Smith 2001).

There is a strong particle size dependency with respect to the occurrence and light scattering impact of inorganic tripton. Large inorganic particles (e.g., >10 μm diameter) settle rapidly because of their density, and thus do not contribute substantially to the particle populations of lacustrine water columns (Davies-Colley and Smith 2001). The most efficient light scattering (e.g., normalized for mass) mineral particles fall in the diameter range of 0.2 to 10 μm, with peak efficiency at 1.1 to 1.2 μm (Kirk 1994; Davies-Colley and Smith 2001) for the most common mineral particles (e.g., clay minerals and quartz). As a result of the combined effects of deposition and light scattering efficiency, mineral particles in the range of 1 to 6 μm dominate light scattering (i.e., T_n) by inorganic tripton in the vast majority of natural waters (Davies-Colley and Smith 2001; Peng and Effler 2006).

Mathematical models of T_n are desired for impacted water supply lakes and reservoirs to represent sources and processes responsible for high turbidities, to predict transport and fate of turbidity-causing particles, and to guide management deliberations for effective rehabilitation. Efforts to model T_n have been relatively rare (e.g., Findikakis et al. 1980). These have generally been based on suspended solids (SS) modeling (Chapra 1997), with T_n predictions generated through SS simulations based on an empirical T_n versus SS relationship. These empirical functionalities are generally system-specific, and often not particularly strong (Davies-Colley and Smith 2001). This approach for modeling T_n should not be expected to be successful in supporting accurate simulations or to be transferable among different systems. The central problem with this approach is the fundamental differences in the particle size dependencies of **b** and mass concentration.

Further, the time and space scales of interest for the turbidity

[1]Research Engineer, Upstate Freshwater Institute, P.O. Box 506, Syracuse, NY, 13214. E-mail: rkgelda@upstatefreshwater.org

[2]Research Engineer, Upstate Freshwater Institute, P.O. Box 506, Syracuse, NY, 13214. E-mail: sweffler@upstatefreshwater.org

Note. Discussion open until July 1, 2007. Separate discussions must be submitted for individual papers. To extend the closing date by one month, a written request must be filed with the ASCE Managing Editor. The manuscript for this paper was submitted for review and possible publication on April 27, 2005; approved on June 15, 2006. This paper is part of the ***Journal of Environmental Engineering***, Vol. 133, No. 2, February 1, 2007. ©ASCE, ISSN 0733-9372/2007/2-139–148/$25.00.

issue are generally finer than have been considered for suspended solids. Seasonal or longer time scales, with limited vertical segmentation (e.g., epilimnion versus hypolimnion), have usually been adopted in SS models (Chapra 1997). Water suppliers are required to deliver low T_n water essentially continuously, and thus are concerned with the effects of short-term perturbations, such as runoff and resuspension events that supply substantial quantities of particles over relatively brief intervals (Bloesch 1995; Longabucco and Raferty 1998). Further, spatial details of manifested impact are important within the context of the locations of water supply withdrawals (Effler et al. 2006b). Turbidity models with these time and space scale attributes have not been reported. Assessment of impacts of runoff events on T_n in many reservoirs is complicated by complex spatial patterns associated with the common occurrence of longitudinal gradients (Thornton et al. 1990) and the plunging inflow, or density current, phenomenon (Martin and McCutcheon 1999). These features place special demands on monitoring programs, that are intended to specify driving conditions and patterns in the model state variables (e.g., T_n) to support model testing, as well as for a hydrodynamic submodel to simulate these transport features.

This paper documents the development and testing of a T_n model for a water supply reservoir, where inorganic tripton dominates T_n, that is based on optical, rather than mass concentration, characteristics of particles. Model testing is supported by detailed measurements of the dynamics of tributary and meteorological drivers and patterns of a surrogate metric of **b** (and T_n) within the reservoir for multiple runoff events. Potential structural additions to the model are considered within the context of mechanistic completeness, and required measurements of forcing conditions and state variables.

Study System

Setting

Schoharie Reservoir is located (latitude 42°23′ N; longitude 74°26′ W) in the Catskill Mountains of southeastern New York, approximately 190 km from New York City (NYC) (Fig. 1). This reservoir, initially filled in 1927, is part of a network of 19 reservoirs that supplies drinking water to 9 million people in the NYC area. The impoundment is 8 km long, has a maximum width of 1 km, and lacks dendritic complexities. When full, the reservoir has a volume of 79×10^6 m^3, a surface area of 4.6 km^2, and a maximum depth of 40 m. However, these morphometric features vary seasonally and year-to-year associated with drawdown of the surface (water surface elevation; WSE, m) in response to withdrawals for the water supply and natural variations in runoff. The reservoir has a dimictic density stratification regime, and it flushes about 10 times per year, on a completely mixed basis. This is an upstream reservoir in NYC's system, as water withdrawn for the water supply travels through an intervening stream and two reservoirs before delivery to NYC.

The main tributary of the reservoir, Schoharie Creek, drains about 75% of the watershed, and enters the reservoir at its southern end (Fig. 1). Since the last glaciation Schoharie Creek and its tributaries have directly contacted glacial and fluvial sediments along much of their drainage ways. These fine sediments are exposed along meander bends and channel troughs that cause high concentrations of suspended material and turbidity in the stream during high runoff events (Smith 2002). The suspended particles of this tributary are primarily inorganic, composed primarily of

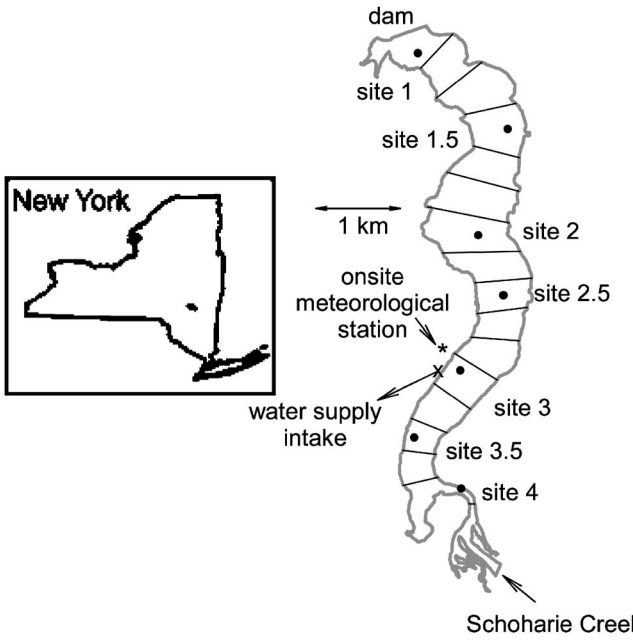

Fig. 1. Schoharie Reservoir, with water supply intake, Schoharie Creek, reservoir monitoring sites, model segments, and location within New York

clay minerals, and regulate T_n levels in the water column of the reservoir (Peng et al. 2004). This case of dominance of turbidity by inorganic tripton is broadly occurring throughout the reservoirs of the NYC water supply (Effler et al. 2002), and in many lakes and other reservoirs (Kirk 1994).

Turbidity Impacts from Runoff Events

The study interval of 2003 (May through October) included 12 runoff events that represent a wide range of stream flow, with recurrence frequencies for Schoharie Creek that extended from 33 yr^{-1} (minor) to 1 yr^{-1} (major; Table 1). The reservoir remained

Table 1. Characteristics of and Model Performance for Twelve Runoff Events for Schoharie Creek for the April–October Interval of 2003

Event[a] no.	Runoff event[b] vol. ($m^3\times10^7$)	Peak in-reservoir $\mathbf{c}_{660}$	RMSE (RMSEN) No. of components 1	2	3
1	0.48	3.7	0.5(13)	0.4(10)	0.5(14)
2	0.41	3.6	0.8(21)	0.6(16)	0.8(23)
3	1.61	8.2	1.4(18)	1.1(13)	1.2(15)
4	1.12	7.0	1.1(15)	0.9(13)	1.0(15)
5	0.18	12.1	1.5(12)	1.1(9)	1.2(10)
6	0.88	7.7	2.2(29)	1.4(18)	1.0(13)
7	1.88	20.1	3.5(17)	2.5(12)	2.1(10)
8	1.95	12.3	3.3(27)	2.1(17)	1.7(14)
9	0.74	12.3	3.2(26)	2.3(18)	1.8(15)
10	0.62	72.8	15.1(21)	14.6(20)	14.8(20)
11	1.57	72.8	11.8(16)	10.9(15)	10.7(15)
12	3.23	79.4	6.5(8)	6.7(8)	7.4(9)

[a]See Fig. 2(a).

[b]From Effler et al. (2006b).

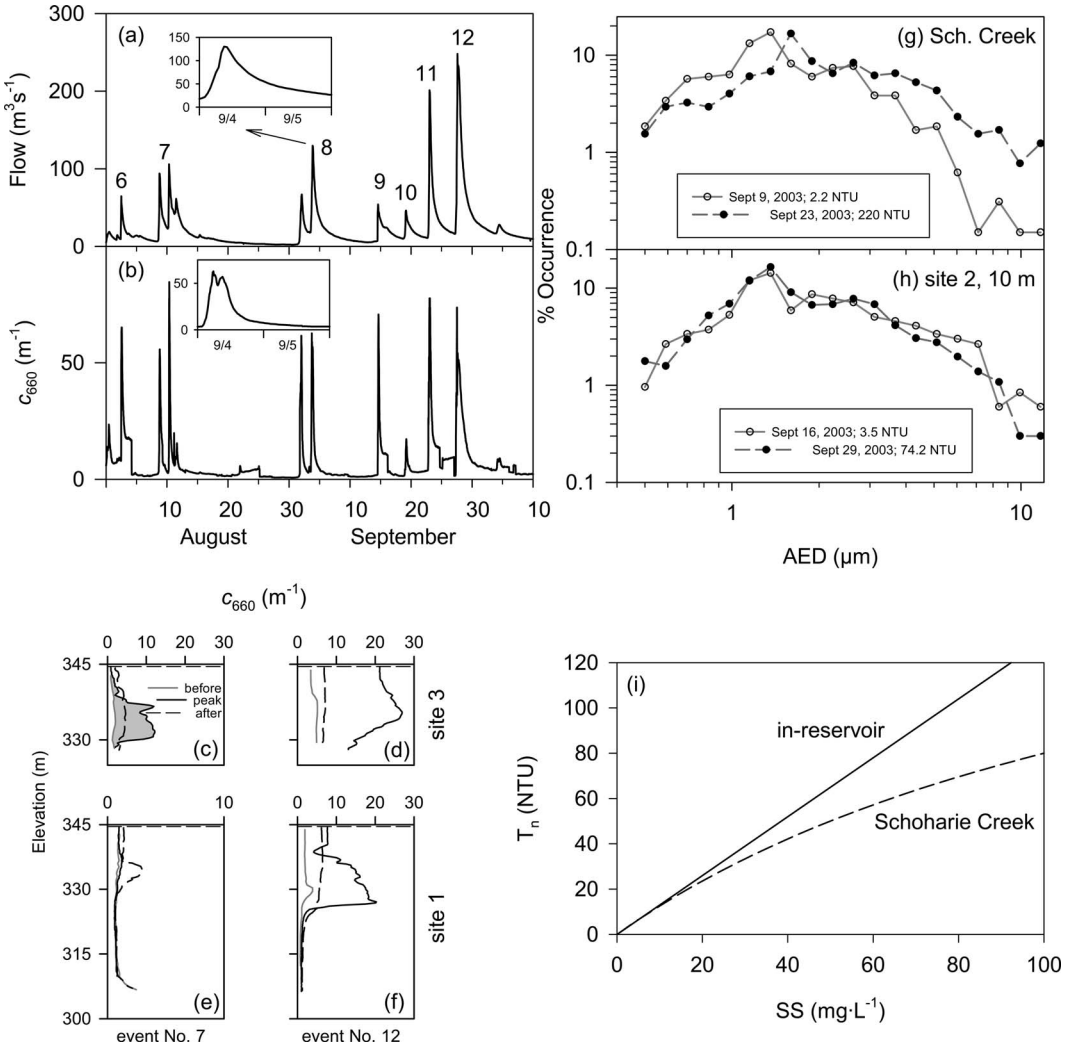

Fig. 2. Selected runoff events for Schoharie Creek and features of turbidity ($\mathbf{c}_{660}$) impacts on Schoharie Reservoir: (a) hydrographs for creek in August and September of 2003, with seven runoff events (Nos. 6–12; inset increased resolution of No. 8); (b) corresponding time-series of $\mathbf{c}_{660}$ for creek [increased resolution of event No. 8 as inset; adapted from Effler et al. (2006b)]; (c) reservoir vertical profiles of $\mathbf{c}_{660}$ for August 8 (before), 12 (peak) and 15 (after) at Site 3, bracketing runoff event No. 7 (adapted from Effler et al. 2006b; peak impact shown as shaded area between the before and peak impact profiles, $\mathbf{c}_{660/Z}$); (d) reservoir vertical profiles of $\mathbf{c}_{660}$ for September 27 (before), October 1 (peak) and 7 (after) at Site 3, bracketing runoff event No. 12; (e) reservoir vertical profiles of $\mathbf{c}_{660}$ for August 8, 12, and 15 at Site 1; (f) reservoir vertical profiles of $\mathbf{c}_{660}$ for September 27, October 1 and 7 at Site 1; (g) particle size distributions for inorganic particles in creek for low and high turbidity conditions; (h) particle size distributions for inorganic particles in the reservoir for low and high turbidity conditions; and (i) relationships between turbidity (T_n) and SS in reservoir and creek

nearly full throughout the study interval. High frequency monitoring of another surrogate of **b**, the beam attenuation coefficient at a wavelength (λ) of 660 nm ($\mathbf{c}_{660}$), in Schoharie Creek documented the delivery of large quantities of turbid water from this tributary during runoff events (O'Donnell and Effler 2006), as illustrated here for events (Nos. 6–12) in August and September of 2003 [e.g., Figs. 2(a and b)]. Levels of light scattering (e.g., $\mathbf{c}_{660}$) increase in this stream as flow (Q) increases (O'Donnell and Effler 2006). The creek generally enters as a turbid density current, or plunging inflow, over the summer through fall interval (Effler et al. 2006b). Accordingly, the relatively dense (cooler; O'Donnell and Effler 2006) stream plunges and travels along the sloping bottom of upstream portions of the reservoir as an underflow and separates from the bottom further downstream, where the density of the underflow equals that of the water column, and enters into that layer as an interflow (e.g., Martin and McCutcheon 1999).

Conspicuous signatures of elevated light scattering are imparted to the water column of the reservoir in response to the turbid water inputs associated with runoff events, as illustrated for two events (Nos. 7 and 12; Table 1) at two sites (Figs. 1) along the major axis of the basin [Figs. 2(c–f)]. The increases in $\mathbf{c}_{660}$ were manifested in sub-surface stratified layers associated with the density current phenomenon (Effler et al. 2006b). Impacts are greater for larger runoff events [e.g., compare Figs. 2(c and e) versus Figs. 2(d and f)], and in up-reservoir versus down-reservoir portions of the reservoir for moderate events [e.g., Figs. 2(c and d) versus Figs. 2(e and f)]. Lateral variations in impact are minor and brief by comparison (Effler et al. 2006b). Levels of light scattering in the reservoir diminish substantially within several days following events [Figs. 2(c–f)], indicating the operation of a loss process(es). A parallel sediment trap program established deposition as an important loss pathway for particles received during runoff events (Effler et al. 2006a).

The size distribution of suspended inorganic particles is shifted to greater contributions by larger particles in Schoharie Creek during high runoff events when levels of light scattering are elevated [(Fig. 2(g)]. In contrast, the particle size distribution of the reservoir water column remains comparatively unchanged over a broad range of light scattering [Fig. 2(h)]. As a result of this disparity in size distribution, the light scattering (e.g., T_n) versus SS relationships for this tributary and the reservoir diverge at elevated levels, with relatively less T_n per unit SS in the stream [Fig. 2(i)].

Modeling

Transport Submodel

The conspicuous patterns of impacts of elevated light scattering documented vertically and along the major axis of the reservoir following runoff events [Figs. 2(c–f)] dictate the need for a two-dimensional hydrodynamic/transport submodel that can represent longitudinal gradients and the behavior of density currents. The hydrodynamic/transport submodel of CE-QUAL-W2, a dynamic, laterally averaged two-dimensional model (Cole and Wells 2002), was adopted. This model is based on the finite-difference solution of partial differential equations for laterally averaged fluid motion and mass transport. The model's equations that describe horizontal momentum, free water surface elevation, hydrostatic pressure, continuity, equation of state, and constituent transport, have been presented previously (Chung and Gu 1998; Cole and Wells 2002). The model assumes that vertical velocities are sufficiently small to allow the vertical momentum equations to be simplified to the hydrostatic equation. The heat budget of the model includes terms for evaporative heat loss, short- and long-wave radiation, convection, conduction and back radiation (Cole and Wells 2002). The model has been applied to a number of systems and issues (e.g., Gelda et al. 1998; Hanna et al. 1999; Gelda and Effler 2002), including simulation of the behavior of density currents (Chung and Gu 1998; Ahlfed et al. 2003), though levels of light scattering have not been considered in those applications. The model represents Schoharie Reservoir in the form of a grid of cells with 17 longitudinal segments (Fig. 1) and vertical layers 1 m thick. Morphometric features of the grid, including dimensions of the layers within the various longitudinal segments, were based on an analysis with ArcInfo (ESRI, Redlands, Calif.) software of a digitized bathymetric map developed from a survey conducted in 1997. Features of the outflow structures are represented, including spillway length, and depths of the water supply withdrawal and dam outlet(s). Inflows and outflows directly enter or exit model segments according to their depths and location. Required inputs to drive the submodel include meteorological conditions (air temperature, dewpoint temperature, wind speed and direction, and solar radiation), the light attenuation coefficient for downwelling irradiance, outflows, and inflow temperature. The model has six coefficients that may be adjusted in the calibration process, though values generally do not vary greatly among systems. The model has been validated for the simulation of the seasonal hydrothermal density stratification regime of Schoharie Reservoir for 14 y (Gelda and Effler 2006), and for the behavior of density currents (based on specific conductance as a conservative tracer) during the 2003 study period.

Modeling Turbidity

The alternative of simulating T_n indirectly through mass balance modeling of SS has been rejected here for both conceptual and practical reasons. First, because larger sized particles make greater contributions to the particle assemblage during high runoff events in the primary tributary than in the water column of the reservoir [Figs. 2(g and h)], the SS approach is fundamentally flawed. Accordingly, the SS approach would result in systematically false high loads within the context of reservoir T_n (light scattering) levels. Apparently, many of the larger particles mobilized in the stream during the high runoff interval are deposited before reaching lacustrine portions of the reservoir. This size sorting process operates widely in reservoirs, manifested as higher sediment deposition (Effler et al. 2001; Effler and Matthews 2004) and accumulation rates and greater contributions by coarser sediments (Pemberton and Blanton 1980) in riverine and transition zones of reservoirs. Further, practical limitations in sampling and analysis for SS compromise resolution of loading and in-reservoir impacts associated with transient runoff events. Direct measurements of a surrogate metric of **b** with appropriate modern instrumentation, as implemented here (subsequently), provides much greater resolution of patterns in time and space to support model testing.

This turbidity model is instead based on mass balance-type modeling of a surrogate metric of **b**, an approach that is supported by the additive character of components and sources of **b** (Davies-Colley et al. 1993). Implicit in this approach is the recognition that light scattering is regulated by characteristics of the particles of the water column, which in natural systems is heterogeneous with respect to size and often composition. The beam attenuation coefficient, **c** is defined by the following summation

$$\mathbf{c} = \mathbf{a} + \mathbf{b} \tag{1}$$

where **a** is the absorption coefficient (m^{-1}). $\mathbf{a}_{660}$ is only ~3 to 6% of $\mathbf{c}_{660}$, and **b** does not vary greatly with λ (Babin et al. 2003), supporting $\mathbf{c}_{660}$ as a surrogate measure of **b**. The value of $\mathbf{c}_{660}$ (**c** is also additive; Davies-Colley et al. 1993) is selected as the model state variable instead of T_n. This choice was also based on both conceptual and practical considerations. Several investigators have indicated that **c** has advantages over T_n as a measure of the magnitude of "turbidity" on scientific grounds (McCarthy et al. 1974; Davies-Colley and Smith 2001). Instruments that measure **c** are subject to absolute calibration, while T_n calibrations are based on an arbitrary standard (Davies-Colley and Smith 2001). Further, T_n values depend to some extent on the particular nephelometer used (Letterman et al. 2004). The $\mathbf{c}_{660}$ metric has the additional advantage of providing more complete spatial resolution (0.25 m vertically at multiple longitudinal positions) of light scattering levels in the reservoir, through implementation of rapid profiling field instrumentation (Effler et al. 2006b). Further, field measurements avoid potential biases from systematic changes associated with the unavoidable delay of laboratory analyses (e.g., flocculation; Effler et al. 2006b). Predictions of $\mathbf{c}_{660}$ can be converted to T_n values (Hach 2100 AN) for this reservoir according to the following linear relationship (Effler et al. 2006b)

$$T_n = 2.5 \cdot \mathbf{c}_{660} \tag{2}$$

Adoption of a light scattering metric instead of SS as the model state variable eliminates the substantial variability and uncertainty that accompanies the representation of light scattering by SS, as-

Table 2. Values of Fractions and Settling Velocities (Adjusted for Temperature), for Selected Single and Multiple Component $\mathbf{c}_{660}$ Models, with Calculated Particle Diameters

Model component	Fractions (%)	Settling vel. ($m\ d^{-1}$)	Diameter (μm)
1	100	1	4.17
2	35, 65	0.01, 3	0.42, 7.21
3	20, 45, 35	0.01, 2.5, 5	0.42, 6.59, 9.31

sociated with the different particle size dependencies of these measures.

The only kinetic process represented in the turbidity model is a first order loss due to settling, as specified by the settling velocity, v ($m\ d^{-1}$). The effect of settling has been represented in three ways. The simplest approach applies a single value of v to the entire $\mathbf{c}_{660}$ pool. The two more complex representations partition the pool into two and three fractions, respectively, each with a different value of v (Table 2). Values of v and the partitioning of the $\mathbf{c}_{660}$ into multiple fractions were determined by model calibration. These different representations essentially treat the settling loss pathway for $\mathbf{c}_{660}$ as being regulated by either a single lumped particle size class or multiple size classes.

Supporting Data and Development of Inputs

The hydrology of the reservoir is well quantified by comprehensive monitoring of inflows and outflows (United States Geologic Survey) and water surface elevation [WSE; New York City Department of Environmental Protection (NYCDEP)]. Ninety-five percent of the reservoir's watershed is gauged (Schoharie Creek and two smaller tributaries). Measurements reported at a time step of 1 h are used here. Ungauged inflows were assumed to have dynamics that tracked those of Schoharie Creek (unpublished data, NYCDEP). Outflows and WSE values were specified at this time step, as the daily average values. Meteorological inputs for the transport submodel were specified at a 20 min time step, based on measurements made at a position along the reservoir's main axis on a monitoring platform located about 2.5 km north of the mouth of Schoharie Creek (Fig. 1). Hourly measurements of temperature (T, °C; accuracy ±0.15 °C, resolution 0.01 °C) and $\mathbf{c}_{660}$ (accuracy ±0.30 m^{-1}, resolution of 0.03 m^{-1}) were made with calibrated instrumentation near the mouth of Schoharie Creek for most of the study period.

Reservoir measurements of T (accuracy ±0.002 °C, resolution 0.003 °C) and $\mathbf{c}_{660}$ (accuracy ±0.30 m^{-1}, resolution 0.03 m^{-1}) were collected with field instrumentation on 42 occasions over the study period. Weekly measurements were made at four long-term monitoring sites (Nos. 1–4) along the main axis of the reservoir, which extend nearly its entire length (Fig. 1). Additional monitoring was conducted during and following runoff events starting in early June (events Nos. 3–12, Table 1). All runoff event-based monitoring included at least 3 additional sites along the main axis, located approximately mid-way between the long-term sites (Nos. 1.5, 2.5, and 3.5; Fig. 1). The measurements of T and $\mathbf{c}_{660}$ were made with rapid profiling instrumentation (Effler et al. 2006b). Eight measurements per second were collected for both parameters during profiling and stored in the instrument's data logger. The instrument was lowered on a cable at a rate of ~0.5 $m\ s^{-1}$; i.e., approximately 16 measurements were made with each sensor over each meter of depth. Measurements ($n \sim 4$) within 0.25 m intervals were averaged, producing detailed vertical profiles. Measurements at the multiple sites were completed within 4 h.

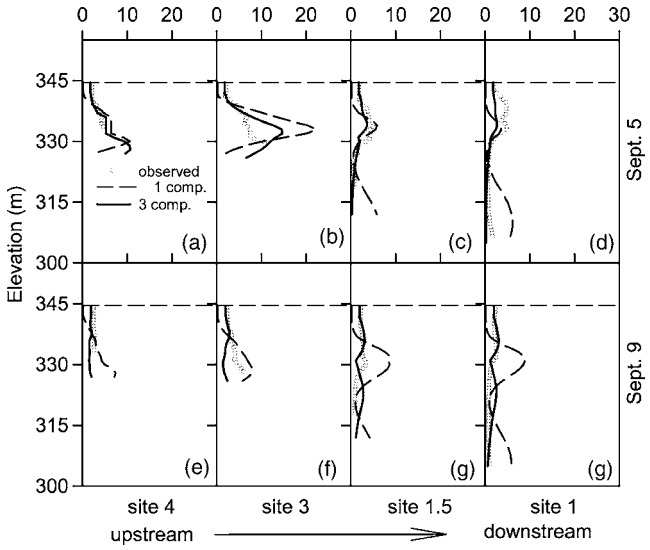

Fig. 3. Performance of model for Schoharie Reservoir for an early September runoff event (No. 8) as comparisons of predicted and observed vertical profiles of $\mathbf{c}_{660}$ according to monitored sites (see Fig. 1); for September 5 (a–d) and September 9 (e–h). Progression from upstream to downstream moves left to right.

Setup, Testing and Evaluation of Model Performance

The model's autostepping algorithm (Cole and Wells 2002) calculates a maximum time-step, within a specified range, based on hydrodynamic numerical stability requirements and uses a fraction of this value for the actual time-step. The minimum and maximum time-steps used were 1 s and 1 h, respectively. The model was initialized according to the measurements of May 6. The predictions presented here result from continuous simulations over the entire study interval (i.e., through October), a much more rigorous test compared to multiple shorter term simulations that would depend on respecification of initial conditions before each of the runoff events.

Model performance was evaluated both qualitatively, through analysis of graphical presentations, and quantitatively, based on statistical comparisons of observations and predictions. Salient features of the impact of runoff events on reservoir light scattering levels considered were: (1) peak levels following events; (2) vertical patterns; (3) longitudinal patterns; and (4) attenuation/diminishment following events. A quantitative basis of model evaluation was the root-mean-square error (RMSE) statistic. RMSE is statistically well behaved (e.g., Thomann 1982), indicating the average error between observations and predictions; lower values generally reflect better performance. The manner of application of the RMSE analysis reflects the emphasis on impact of runoff events. Analyses were conducted over intervals extending from the peak documented impact of an event to 7 d later. These values were "normalized" by the $\mathbf{c}_{660}$ maximum (RMSEN) observed for each event to depict relative performance across the wide range of magnitudes of runoff events and impacts.

Model Performance and Sensitivity

Graphical representations of model performance in simulating $\mathbf{c}_{660}$ levels in the reservoir are presented in three formats: (1) detailed vertical profiles for the four monitored sites for two days during event No. 8 (Fig. 3); (2) time series for three depth inter-

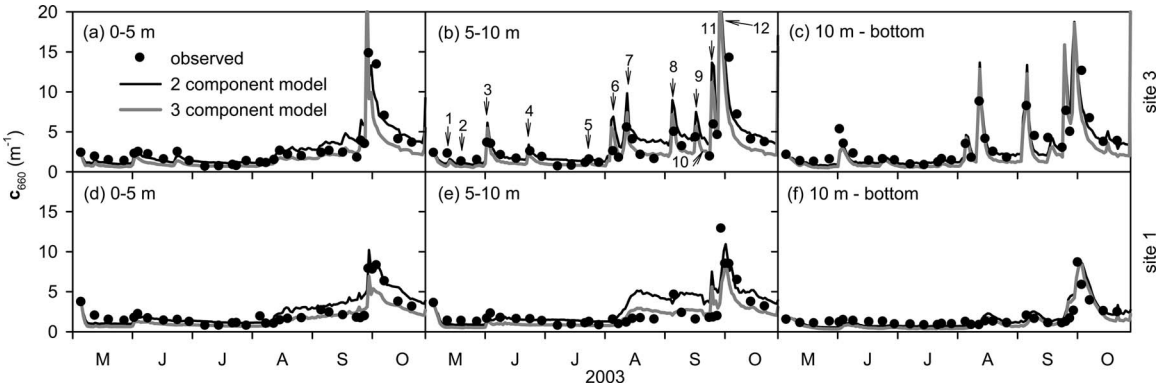

Fig. 4. Performance of model for Schoharie Reservoir as comparisons of predicted and observed time series of $\mathbf{c}_{660}$ for three vertical segments (volume-weighted) for two monitoring sites (a) 0–5 m, Site 3; (b) 5–10 m, Site 3; (c) 10 m–bottom, Site 3; (d) 0–5 m, Site 1; (e) 5–10 m, Site 1; and (f) 10 m–bottom, Site 1

vals of the water column (0–5 m, 5–10 m, and 10 m–bottom) of volume-weighted values at two reservoir sites for the entire study (Fig. 4); and (3) longitudinal and vertical patterns as iso-$\mathbf{c}_{660}$ lines for two days during Event No. 7 (Fig. 5). Representations of performance in terms of the RMSE and RMSEN statistics are presented in tabular form for each of the runoff events and representations of component fractions and settling (Table 1). Comparison of the one and three component $\mathbf{c}_{660}$ models is presented in the format of vertical profiles (Fig. 3), while performance of the two and three component representations is contrasted in the time series simulations for the three strata (Fig. 4). The performance of the multi-component models was generally superior to the single component representation for the overall study; e.g., the average RMSEN for the one component model was 18.6% compared to 14.0% and 14.4% for the two and three component approaches. Graphical comparisons further support this position

Both the one and three component models performed well in simulating the vertical position of the $\mathbf{c}_{660}$ maxima along the longitudinal axis of the reservoir during the peak impact of Event No. 8 [September 5; Figs. 3(a–d)]. Levels of $\mathbf{c}_{660}$ were overpredicted at Site 3 [Fig. 3(b)], but the attenuation of impact in downstream portions of the reservoir for this modest runoff event (Table 1) was well simulated for the three component model [Figs. 3(c and d)]. These performance features, immediately following the event, were largely controlled by the hydrodynamic transport model. The predictions presented for the single component $\mathbf{c}_{660}$ model correspond to a value of $v=1$ m d^{-1} (Table 2), from calibration that focused on performance within the depths of the maxima. Systematic short-comings in performance emerged for this simple kinetic framework even during peak impact. Levels of $\mathbf{c}_{660}$ were underpredicted in the near-surface waters along the entire reservoir [Figs. 3(a–d)] and overpredicted, as a second maximum, in deeper layers in downstream segments [Figs. 3(c and d)]. No single value of v could eliminate both of these shortcomings. Performance of the single component approach worsened four days later (September 9) as impact diminished and kinetics (deposition) became relatively more important following the initial event driven transport [Figs. 3(e–h)]. The extent of diminishment in subsurface layers was underpredicted throughout the reservoir, as manifested by false high predictions of $\mathbf{c}_{660}$ at depth of ~15 m (elevation=330 m). Levels in the surface waters continued to be underpredicted and those at depths>30 m (elevation 315 m) were overpredicted.

Vertical features of performance improved substantially with

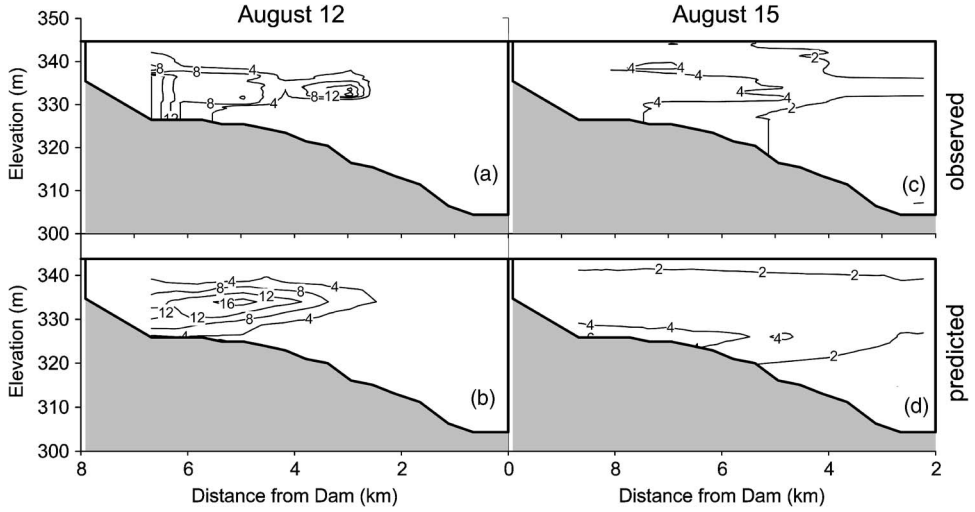

Fig. 5. Performance of model for Schoharie Reservoir as comparisons of predicted and observed longitudinal patterns of $\mathbf{c}_{660}$ levels along its major axis (event No. 7): (a) observed August 12; (b) predicted August 12; (c) observed August 15; and (d) predicted August 15

both the two and three component frameworks, as illustrated here for the three component model [Figs. 3(a–h)]. Values of the fractions and the corresponding v for the multiple component models determined through calibration are presented tabularly, along with corresponding particle diameters calculated according to Stokes law (temperature adjusted; Reynolds Number $Re \ll 1$) for the spherical and inorganic (i.e., density ~ 2.6 g cm^{-3}) particle assumptions (Table 2). Qualitatively the multiple component approach corresponds to a persistent (i.e., slow settling) fraction and a single or two rapidly settling fraction(s) of particles responsible for light scattering ($\mathbf{c}_{660}$). This approach resulted in much better simulation of levels in surface waters and in deep layers in downstream portions of the reservoir for both peak impact and diminishing effect intervals (Fig. 3), and in terms of overall statistical metrics of performance (Table 1). The three component model somewhat underpredicted $\mathbf{c}_{660}$ at depths >10 m in upstream portions of the reservoir for September 9.

The time series representation of model performance (Fig. 4) is valuable in considering temporal features within the context of the entire study period. These time series of observations and simulations also serve to demonstrate the distinct temporal and spatial patterns imparted by the runoff events of the study period (Table 1). Attenuation of the impact in both time and space (Site 3 versus Site 1) is clearly evident. These patterns were generally predicted by both the two and three component representations for the three strata at both upstream (Site 3) and downstream (Site 1) monitored locations. The model predictions explained 65 to 95% of the observed temporal variations within the defined strata ($n=6$) of these two sites (Fig. 4). The two component model performed generally better over the May through July period, an interval of lower runoff and smaller events. However, the three component model tracked observations closer in August and September when severe runoff events occurred; an exception was the lower stratum at Site 3 [Fig. 4(c)]. Improvements compared to the two component model were most noteworthy in the mid-depth stratum [Figs. 4(b and e)]. However, the two component model performed better for the largest runoff event (No. 12, Table 1) and subsequent diminishment. The three component model is favored for Schoharie Reservoir primarily because of its overall better performance.

The two-dimensional patterns of $\mathbf{c}_{660}$ imparted by runoff event No. 7 on August 12, and subsequent diminishment of impact on August 15, were generally simulated well by the two component model [Figs. 5(a–d)]. The longitudinal limits of impact of the event were well predicted for August 12, though the difference in the location of maximum $\mathbf{c}_{660}$ indicates a modest over prediction of travel time of the turbid plume [Figs. 5(a and b)]. The smaller number of monitored sites compared to model segments (Fig. 1) is a source of differences for predictions and observations in the longitudinal dimension for this contour representation of performance. The extent of diminishment of impact in mid-reservoir areas on August 15 was only slightly overpredicted [Figs. 5(c and d)].

The magnitude of the RMSE of model predictions generally increased with the magnitude of impact imparted by a runoff event, as reflected by the peak $\mathbf{c}_{660}$ observed in the reservoir (Table 1). However, when performance is considered relative to this metric of event impact, as RMSEN, much greater uniformity is indicated. For example, the RMSEN for the two component model ranged from 8 to 20% for the 12 events (Table 1) and the coefficient of variation for this performance metric for the events was only 27%. According to the RMSEN metric, performance of the multi-component models was the best for Events 5 and 12 and the worst for Event 10. Model predictions were found to be sensitive to the specified fractions and corresponding settling velocities of the components of $\mathbf{c}_{660}$, and frequency of tributary measurements of $\mathbf{c}_{660}$ during events that specify external inputs.

Advancement in Turbidity Modeling and Model Structure Issues

A turbidity ($\mathbf{c}_{660}$) model has been developed and successfully tested that for the first time meets the demanding temporal and spatial needs of water supply lakes and reservoirs. Advancements on the problems of turbidity modeling have been made with respect to: (1) the selection of an appropriate state variable(s); (2) development of appropriate specifications of patterns, in time and space, of forcing conditions and in-reservoir conditions to support model testing; and (3) the evolution to a multiple-turbidity (particle)—class kinetic framework. The approaches used here are expected to be applicable for many other systems where event-based terrigenous inputs are important in regulating turbidity patterns. Further, the two-dimensional transport framework adopted here will be appropriate for many reservoirs and lakes (Martin and McCutcheon 1999). It is extremely unlikely the demonstrated capabilities of the model could be met with an approach that instead was based on SS, for both conceptual and practical reasons. Event-based sampling of the primary source(s) of turbidity and comprehensive spatial monitoring of a surrogate of **b** were necessary to support testing.

Further, it appears likely that at least two turbidity classes will be required in most if not all lakes and reservoirs. This last point deserves expansion. The values of v arrived at by calibration, correspond to particle diameters (assuming spherical) of approximately 0.42 and ≥ 6.6 μm according to Stokes law (Table 2). The larger sizes represent much lower contributions (e.g., $\leq 1\%$) of the measured particle population of the water column [Fig. 2(h)] than the fractions determined from calibration (Table 2). The effective size of these particles may be even greater, and thus their occurrence even rarer than indicated by Stokes law estimates (Table 2), because of the platelike (i.e., nonspherical) features of many (e.g., clay) of the particles (Peng et al. 2004). The need for such a high settling velocity indicates the operation of particle aggregation is effectively embedded within the rapid settling fractions. Aggregation/coagulation is generally considered to be a ubiquitous phenomenon that is known to be promoted by high concentrations of divalent cations and low dissolved organic carbon (DOC) levels (O'Melia 1980; Weilenmann et al. 1989). Given the rather low divalent cation (e.g., calcium ~ 5 mg L^{-1}; NYCDEP 2002) and common DOC levels (~ 1.7 mg L^{-1}, unpublished data, Upstate Freshwater Institute) that prevail in Schoharie Reservoir, it is likely that the effects of this process will need to be accommodated in most systems (e.g., O'Melia 1985). This may be represented implicitly through specification of appropriate values of v (i.e., through model calibration), as described here, or through explicit representation of the aggregation process (e.g., O'Melia 1980; Weilenmann et al. 1989; Fig. 6). Even higher values of v and/or shifts to greater contributions to turbidity by the more rapidly settling fractions are to be expected for systems where the chemical environment promotes aggregation processes (e.g., higher divalent ion and lower DOC concentrations; O'Melia 1980; Weilenmann et al. 1989).

Explicit representation of particle aggregation would require the consideration of multiple particle size classes as model state variables, within the context of a more complex particle-based

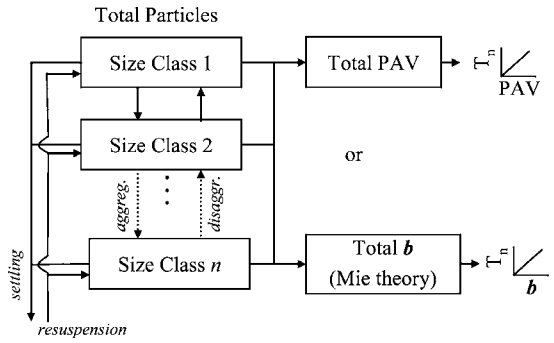

Fig. 6. Conceptual framework for a mechanistically more robust turbidity model based on multiple particle size classes

turbidity model (Fig. 6), by describing the effects of collision frequency and collision efficiency (α), the fraction of particle collisions that results in formation of an aggregate (O'Melia 1985). Such a framework also has appeal as more rigorously fitting the constraints of mass balance, compared to the quasi-mass balance features of the $\mathbf{c}_{660}$ approach utilized here. A model framework has been developed for lakes and reservoirs that represents aggregation, and accommodates loading and deposition of particles (O'Melia 1980, 1985). The model has been applied to several hypothetical cases to illustrate the interplay between the processes, and particularly the importance of aggregation and related regulating processes (O'Melia 1980; O'Melia and Bowman 1984; O'Melia 1985). Further, some guidance on specification of values of α has been developed in laboratory experiments for a range of water chemistry conditions known to influence particle stability (Gibbs 1983). However, adequate data, particularly in the form of detailed particle information (composition, concentration and size distribution) in loads and within downstream reservoirs and lakes, have not been available to rigorously test these frameworks. Particle counting and sizing instrumentation, including in situ measurement capabilities (Agrawal and Pottsmith 2000), is becoming increasingly available, and will promote testing of such frameworks in the future.

The disaggregation process, the break-up of flocculated particles, is also acknowledged to be ubiquitous (Lick and Lick 1988). Inclusion of this process in a particle model (e.g., Fig. 6) would result in a more general and complete representation of particle dynamics. However, it has received far less research attention, and widely accepted quantitative representations for real ecosystems are generally lacking (Jackson and Burd 1998). Operationally, omission of this process would result in aggregation representing a net loss of particles.

Resuspension, the reconveying of particles to the water column induced by water motion (Bloesch 1995; Lick et al. 1995), is a ubiquitous internal source of particles. Thus its inclusion within the model framework (Fig. 6) would represent a more general, and potentially more powerful, tool. However, the relative importance of this source and the regulating driver(s) and mediating processes (e.g., surface waves, internal waves, scour in riverine zones) is highly system specific (Bloesch 1995). Drawdown of a reservoir surface promotes resuspension in at least two ways. First, portions of the reservoir bottom that were previously below the wave base, where deposited sediment can accumulate, become subject to wave driven resuspension as the water surface drops (Effler and Matthews 2004). Second, drawdown exposes sediment deposits in upstream portions of the reservoir to more riverine (e.g., higher velocities) conditions. The absence of a conspicuous benthic nepheloid layer (Effler et al. 2006b) and features of deposition assessed with sediment traps (Effler et al. 2006a) under the nearly full conditions that prevailed in Schoharie Reservoir over the 2003 study period indicate resuspension was not an important source. This simplification promoted a more rigorous test of the effects of external loading, transport and settling/aggregation. A more robust model, that also includes a resuspension source of turbidity, may be necessary to represent conditions in this reservoir during periods of extensive drawdown.

Commitment to the more complex framework inherent in modeling multiple particle size classes requires predictions of the associated **b** (turbidity or its surrogates). Empirical or mechanistic pathways could be adopted (Fig. 6). The empirical pathway relies on the projected area of particles per unit volume, the morphometric feature most closely coupled to the magnitude of **b** (Treweek and Morgan 1980). Particularly strong relationships, with intercepts approaching zero, have been reported between turbidity and total PAV for systems such as Schoharie Reservoir where inorganic particles are an important to dominant component of **b** (Effler et al. 2002; Peng et al. 2004). However, variations in particle size distribution and composition could compromise such an approach. A more theoretically rigorous approach would adopt Mie theory calculations (e.g., Babin et al. 2003), or related simplifications (Kirk 1994), to predict **b** from particle counts, size distribution, and composition information (Fig. 6).

A test system where inorganic tripton regulates **b** and its surrogates is appropriate to advance and test more robust and complex model frameworks capable of simulating the impacts of runoff events (Fig. 6). Detailed monitoring of particle populations, the conduct of various process studies (e.g., aggregation and resuspension), and the development, testing and application of complex model frameworks (e.g., Fig. 6), serves to advance not only related research but to evaluate alternative simpler frameworks (and supporting programs) with potentially broader management utility. A test system such as Schoharie Reservoir avoids the complexities associated with simulation of the effects of phytoplankton (e.g., Chapra 1997). Yet advancements in approaches for inorganic particles are generally transferable for systems where phytoplankton are also important because of the additivity of the components of **b** (Kirk 1994).

Summary and Recommendations

A model for $\mathbf{c}_{660}$, a surrogate of T_n and **b**, has been developed and successfully tested for a water supply reservoir that experiences conspicuous increases in turbidity, in the form of terrigenous inorganic particles, in response to inputs received in turbid density currents during runoff events. The model and related testing efforts featured: (1) $\mathbf{c}_{660}$ as the model state variable, rather than the systematically flawed gravimetric measure of SS; (2) comprehensive monitoring of tributary and meteorological forcing conditions and in-reservoir temporal and spatial patterns of $\mathbf{c}_{660}$ for multiple runoff events; (3) a two-dimensional (laterally averaged) hydrodynamic submodel that performed well in simulating the transport of density currents through the reservoir; and (4) a partitioning of $\mathbf{c}_{660}$ into slow and rapid settling fractions.

This is the first turbidity model that has been demonstrated to meet the fine temporal and spatial scale needs for a water supply lake or reservoir impacted by runoff events. Treatment of $\mathbf{c}_{660}$ as a single pool, settling at a single settling velocity (v), was found to be an inadequate representation. The high values of v incorpo-

rated in the multiple fraction model relative to the available particle size distribution information provided strong evidence for the operation of aggregation processes. The model performed well in simulating the timing and magnitude of $\mathbf{c}_{660}$ peaks in the reservoir soon after runoff events, the distinct vertical and longitudinal patterns in this metric, the diminishment following events, and the dependence of the impact on the magnitude of the runoff event. The framework and approach is expected to be transferable to many water supply reservoirs and lakes. Exceptions include systems where the resuspension source of turbidity is high relative to direct terrigenous inputs or those where important patterns develop in three dimensions (e.g., three dimensional transport model required) instead of just two.

Further advancements in turbidity modeling should be made to construct more robust and powerful management tools and to serve as an integrator of related research. A broader range of drivers needs to be represented, such as spring runoff events that enter as overflows and runoff events during extensive drawdown. More robust and complex model frameworks would represent multiple particle classes, partitioned according to size and perhaps composition, as state variables, and include explicit representations of the particle aggregation, resuspension, and perhaps light scattering, processes. Theoretical constructs exist for most of these features, but progress has been limited by the lack of adequate characterization of particle populations in real systems and uncertainties in the representation of certain processes. Recent advancements in instrumentation and contemporary understanding of related processes and phenomena make development and testing of such complex frameworks feasible for an appropriate test system(s). These efforts should first focus on a test system where inorganic particles regulate turbidity patterns but where a robust array of the above drivers prevail (e.g., clear and separable signatures from runoff and resuspension events), before addressing the added complexities of also including phytoplankton effects. Integration of advancements from a complex research model into a simpler framework for broader management applications will need to reflect the interplay, and a balance, between model complexity, credibility and utility.

Acknowledgments

Support for this study was provided by the New York City Department of Environmental Protection. Field sampling and measurements were conducted by M. Spada, B. Wagner, and T. Prestigiacomo. D. O'Donnell managed the tributary and meteorological monitoring efforts. S. O'Donnell assisted in data management and modeling efforts. This is contribution No. 240 of the Upstate Freshwater Institute.

References

Agrawal, Y. C., and Pottsmith, H. C. (2000). "Instruments for particle size and settling velocity observations in sediment transport." *Mar. Geol.*, 168, 89–114.

Ahlfeld, D., Joaquin, A., Tobiason, J., and Mas, D. (2003). "Case study: Impact of reservoir stratification on interflow travel time." *J. Hydraul. Eng.*, 129(12), 966–975.

Babin, M., Morel, A., Fournier-Siere, V., Fell, F., and Stramski, D. (2003). "Light scattering properties of marine particles in coastal and open ocean waters as related to the particle mass concentration." *Limnol. Oceanogr.*, 48, 843–859.

Bloesch, J. (1995). "Mechanisms, measurement and importance of sediment resuspension in lakes." *Mar. Freshwater Res.*, 46, 295–304.

Chapra, S. C. (1997). *Surface water-quality modeling*. McGraw-Hill, New York.

Chung, S. W., and Gu, R. (1998). "Two-dimensional simulations of contaminant currents in stratified reservoir." *J. Hydraul. Eng.*, 124(7), 704–711.

Cole, T. M., and Wells, S. A. (2002). "CE-QUAL-W2: A Two-Dimensional, Laterally Averaged, Hydrodynamic and Water Quality Model, Version 3.1." *Instruction Report EL-2002-1*. U.S. Army Engineering and Research Development Center, Vicksburg, Miss.

Davies-Colley, R. J., and Smith, D. G. (2001). "Turbidity, suspended sediment, and water clarity: A review." *J. Am. Water Resour. Assoc.*, 37, 1085–1101.

Davies-Colley, R. J., Vant, W. N., and Smith, D. G. (1993). *Colour and clarity of natural waters*, Ellis Horwood, New York, New York.

Effler, S. W., Matthews (Brooks), C. M., and Matthews, D. A. (2001). "Patterns of gross deposition in reservoirs enriched in inorganic tripton." *Can. J. Fish. Aquat. Sci.*, 58, 2177–2188.

Effler, S. W., and Matthews, D. A. (2004). "Sediment resuspension and drawdown in a water supply reservoir." *J. Am. Water Resour. Assoc.*, 40, 251–264.

Effler, S. W., Matthews, D. A., Kaser, J., Prestigiacomo, A., and Smith, D. G. (2006a). "Runoff event impacts on a water supply reservoir: Suspended solids loading, turbid plume behavior and sediment deposition." *J. Am. Water Resour. Assoc.*, in press.

Effler, S. W., Perkins, M. G., Ohrazda, N., Matthews, D. A., Gelda, R. K., Peng, F., Johnson, D. L., and Stepczuk, C. L. (2002). "Tripton, transparency and light penetration in seven New York reservoirs." *Hydrobiologia*, 468, 213–232.

Effler, S. W., Prestigiacomo, A., Peng, F., Bulygina, K. B., and Smith, D. G. (2006b). "Resolution of turbidity patterns from runoff events in a water supply reservoir, and the advantages of *in situ* beam attenuation measurements." *Lake Reserv. Manage.*, 22, 79–93.

Findikakis, A. N., Locher, F. A., and Ryan, P. J. (1981). "Temperature and turbidity simulation in Spada Lake." *Proc. Symp. Surface Water Impoundments*. American Society of Civil Engineers, New York.

Gelda, R. K., and Effler, S. W. (2002). "A river water quality model for chlorophyll and dissolved oxygen that accommodates zebra mussel metabolism." *Wat. Qual. Eco. Model.*, 1, 271–309.

Gelda, R. K., and Effler, S. W. (2006). "Testing and application of a two-dimensional hydrothermal model for a water supply reservoir: Implications of sedimentation on withdrawal temperatures." *J. Environ. Eng. Sci.*, in press.

Gelda, R. K., Owens, E. M., and Effler, S. W. (1998). "Calibration, verification, and an application of a two-dimensional hydrothermal model [CE-QUAL-W2(t)] for Cannonsville Reservoir." *Lake Reserv. Manage.*, 14, 186–196.

Gibbs, R. G. (1983). "Effect of natural organic coatings on the coagulation of particles." *Environ. Sci. Technol.*, 17, 237–240.

Hanna, R. B., Saito, L., Bartholow, J. M., and Sandelin, J. (1999). "Results of simulated temperature control device operations on in-reservoir and discharge water temperatures using CE-QUAL-W2." *Lake Reserv. Manage.*, 15, 87–102.

Jackson, G. A., and Burd, A. B. (1998). "Aggregation in the marine environment." *Environ. Sci. Technol.*, 19, 2805–2814.

James, R. T., Martin, J., Wool, T., and Wang, P. F. (1997). "A sediment resuspension and water quality model of Lake Okeechobee." *J. Am. Water Resour. Assoc.*, 33, 661–680.

Kirk, J. T. O. (1994). *Light and photosynthesis in aquatic ecosystems*, Cambridge University, London.

Letterman, R. D., Johnson, C. E., and Viswanthan, S. (2004). "Low-level turbidity measurements: A comparison of instruments." *J. Am. Water Works Assoc.*, 96, 125–137.

Lick, W., and Lick, J. (1988). "Aggregation and disaggregation of fine-grained lake sediments." *J. Great Lakes Res.*, 14, 514–523.

Lick, W., Xu, Y. J., and McNeil, J. (1995). "Resuspension properties of sediments from the Fox, Saginaw, and Buffalo Rivers." *J. Great Lakes Res.*, 21, 257–274.

Longabucco, P., and Rafferty, M. R. (1998). "Analysis of material loading to Cannonsville Reservoir: Advantages of event-based sampling." *Lake Reserv. Manage.*, 14, 197–212.

Martin, J. L., and McCutcheon, S. C. (1999). *Hydrodynamics and transport for water quality modeling*, Lewis Publishers, Boca Raton, Fla.

McCarthy, J. C., Pyle, J. E., and Griffin, G. M. (1974). "Light transmissivity, suspended sediments and the legal definitaion of turbidity." *Estur. Coast. Mar. Sci.*, 2, 291–299.

NYCDEP. (2002). "Watershed water quality annual report." New York City Department of Environmental Protection, Valhalla, NY.

O'Donnell, D. M., and Effler, S. W. (2006). "Resolution of impacts of runoff events on a water supply reservoir with a robotic monitoring network." *J. Am. Water Resour. Assoc.* 42, 323–335.

O'Meila, C. R. (1980). "Aquasols: The behavior of small particles in aquatic systems." *Environ. Sci. Technol.*, 14, 1052–1060.

O'Melia, C. R. (1985). "The influence of coagulation and sedimentation on the fate of particles, associated pollutants, and nutrients in lakes." *Chemical processes in lakes*, W. Stumm, ed., Wiley Interscience, New York, NY, 207–224.

O'Meila, C. R., and Bowman, K. S. (1984). "Origins and effects of coagulation in lakes." *Schweiz. Z. Hydrol.*, 46, 64–85.

Pemberton, E. L., and Blanton, J. O., III. (1980). "Procedure for monitoring reservoir sedimentation." *Proc., Symp. Surface Water Impoundments*. ASCE, New York, 1269–1278.

Peng, F., and Effler, S. W. (2006). "Suspended minerogenic particles in a reservoir: Light scattering features from individual particle analysis." *Limnol. Oceanogr.*, in press.

Peng, F., Johnson, D. L., and Effler, S. W. (2004). "Characterization of inorganic particles in selected reservoirs and tributaries of the New York City water supply." *J. Am. Water Resour. Assoc.*, in press.

Phlips, E. J., Aldridge, F. J., Schelske, C. L., and Crisman, T. L. (1995). "Relationships between light availability, chlorophyll *a*, and tripton in a large shallow subtropical lake." *Limnol. Oceanogr.*, 40, 416–421.

Smith, D. G. (2002). "Turbidity in Catskill watershed." New York City Department of Environmental Protection, Division of Drinking Water Quality Control, Bureau of Water Supply, Valhalla, NY.

Thomann, R. V. (1982). "Verification of water quality models." *J. Envir. Engrg. Div.*, 108, 923–940.

Thornton, K. W., Kimmel, B. L., and Payne, F. E. (1990). *Reservoir limnology: Ecological perspectives*, John Wiley and Sons, NY.

Treweek, G. P., and Morgan, J. J. (1980). "Prediction of suspension turbidities from aggregate size distribution." *Particles in water*, M. C. Kavanaugh and J. O. Leckie, eds., Advances in Chemistry Series, No. 189, American Chemical Society, Washington, D.C.

Weilenmann, U., O'Melia, C. R., and Stumm, W. (1989). "Particle transport in lakes: Models and measurements." *Limnol. Oceanogr.*, 34, 1–18.

Wetzel, R. G. (2001). *Limnology: Lake and reservoir ecosystems*, Academic Press, New York.